Quantifying the intra- and inter-subject variability of whole-brain structural networks from diffusion MRI

Colin R. Buchanan[1], Krzysztof Gorgolewski[1], Cyril R. Pernet[2], Amos J. Storkey[1], and Mark E. Bastin[2]
[1]*School of Informatics, University of Edinburgh, Edinburgh, United Kingdom,* [2]*School of Molecular & Clinical Medicine, University of Edinburgh, Edinburgh, United Kingdom*

INTRODUCTION

Connectomics is a recent development in neuroscience that combines diffusion MRI (dMRI) and tractography with the analytical tools of network theory to investigate whole-brain connectivity [1]. Under this paradigm, segmented cortical areas (e.g. Brodmann areas) form the nodes of a network and tractography is used to construct a set of white matters tracts which form the connections of the network. Graph-theoretic measures may then be used to characterize topological patterns of connectivity [2]. Recent studies have demonstrated whole-brain network analysis in healthy volunteers [3,4]. However, whether the connectome approach can consistently reconstruct structural white matter networks and produce robust clinically useful metrics remains an open question. Here we measure the reproducibility of basic graph-theoretic measures obtained from dMRI data using a percentile bootstrap technique. Since these measures are an essential prerequisite for more complex analyses, such as "small-world" measures or the identification of network hubs, their reliability is crucial to the whole connectome approach.

METHODS

Ten healthy volunteers (six female and four male, aged between 50 and 58 years) underwent a dMRI protocol on two separate occasions over an interval of either two or three days. All imaging data was acquired using a GE Signa HDxt 1.5 T (General Electric, Milwaukee, WI, USA) clinical scanner. For the dMRI protocol, single-shot spin-echo echo-planar (EP) diffusion-weighted whole-brain volumes (b = 1000 s mm^{-2}) were acquired in 64 noncollinear directions, along with seven T_2-weighted volumes (b = 0 s mm^{-2}) at 2×2×2 mm resolution. 3D T_1-weighted volumes were also acquired at 1×1.3×1 mm resolution in each session. Using the 3D T_1-weighted volume scans, FreeSurfer [5] was used to perform automated brain extraction, grey and white matter segmentation and parcellation of cortical sulci and gyri. We used the Desikan-Killiany atlas [5], supplemented with the segmentation of 16 sub-cortical grey matter structures [6], resulting in 84 regions-of-interest (ROIs) per subject. Anatomical ROIs were registered from T_1-weighted space to diffusion space (FSL FLIRT), while dMRI volumes were corrected for eddy-current induced distortions and patient motion using affine registration (FSL Eddy Correct). Tractography was then initiated from all voxels within each ROI using the probabilistic index of connectivity (PICo) algorithm [7]. 100 streamlines were initiated from each seed location and constructed from voxel to voxel until terminated by stopping criteria, specifically, curvature exceeding 80 degrees or entering an extra-cerebral voxel or region of cerebrospinal fluid. Cortico-cortical connections were computed by recording tracts found between all ROI pairs in an 84×84 adjacency matrix a, where the entry a_{ij} denotes the connection weight between node i and node j, weighted by the connection probability derived from probabilistic tractography. Each adjacency matrix was normalized by the white matter volume determined from the 3D T_1-weighted volume scan (FreeSurfer) to correct for variation in the number of tracts due to differences in brain volume. Considering the brain as a network of nodes enables use of graph-theoretic measures. For each network we computed: two measures of global connectivity, namely, the *mean node degree* and the *mean node strength*; a global measure of segregation, the *mean clustering coefficient*; and a measure of integration, the *characteristic path length* [2]. Where possible, metrics were computed using weighted variants rather than thresholding or binarising the adjacency matrices. For each of the four metrics we computed the population mean, the average between-subject differences (average differences of each subject against the others), and the within-subject differences (differences between two sessions). A percentile bootstrap on the mean differences with family-wise correction was used to compare the within and between-subject components. Differences between sessions vs. mean differences between subjects were resampled 1000 times and absolute differences for within vs. between-subject obtained. Simultaneous probability coverage was obtained by taking the maximum over each bootstrap. Differences were considered significant if the 95% confidence intervals did not include 0.

RESULTS AND DISCUSSION

Table 1 shows the population mean and the mean between-subject and within-subject differences (expressed as a proportion of the population mean) for the four graph-theoretic measures. Figure 1 shows the estimated pair-wise differences in within-subject vs. between-subject components with 95% confidence intervals. In all four cases, within-subject differences were smaller than between-subject differences. This shows that despite noisy measurements, it is possible to produce highly consistent network metrics across sessions (interscan difference of less than 6% across all measures). For example, though the characteristic path length (average path length between all pairs of nodes) varies little between sessions or individuals it can be computed consistently across sessions. Considering the metrics of connectivity, the small values of both within and between-subject differences for node degree (the count of connecting links to a node), suggests that the "total wiring" varies little between subjects. However, the larger difference in node strength (the sum of the weights of the connecting links) suggests that in general the "strength" of connection varies by ~7% between subjects (assuming a linear relationship between vs. within differences). Computing the small world property from the characteristic path length and clustering coefficient [2], shows, like most connectome studies, that the brain networks of our volunteers have a "small world" architecture (most nodes are not neighbors but can be reached in a small number of steps). As the small word property is the ratio of two reliable measures any measures derived from these metrics will also be reliable. A direct comparison to other dMRI studies is not straightforward due to differences in subject populations, image acquisition and data processing methods. However, our components are broadly similar to the coefficients of variation found in earlier work [4], which used thresholded networks but did not separate between and within-subject variation.

	mean	intersubject diff (%)	interscan diff (%)
mean node degree	57.78	3.88	2.25
mean node strength	1.80	13.10	5.65
characteristic path length	1.19	2.70	1.44
mean clustering coefficie	0.01	13.21	5.24

Table 1: Population mean and mean between-subject and within-subject differences for four global network metrics.

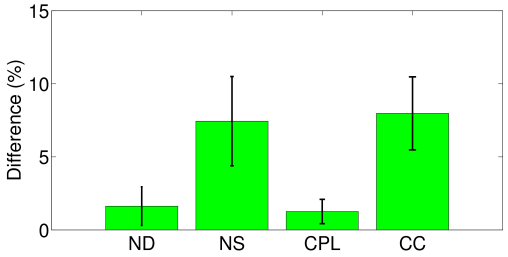

Figure 1: Differences between within-subject and between-subject components and 95% confidence interval estimated by bootstrap resampling, for mean node degree (ND), mean node strength (NS), characteristic path length (CPL) and mean clustering coefficient (CC).

CONCLUSIONS

We have quantified the between and within-subject components of four commonly used graph-theoretic measures of brain connectivity from repeat scans of ten healthy volunteers. Results show that structural differences between individuals are greater than differences due to repeat scanning. Our method produces network metrics consistently between imaging sessions with interscan difference of less than 6%. Our findings and statistical framework may inform the development of network analysis and in turn lead to a better understanding of the topological structure of the brain. Appropriate metrics may then be used to assess brain connectivity between individuals or across populations.

REFERENCES

[1] Sporns et al., PLoS, Comput. Biol., 1(4):e42, 2005. **[2]** Rubinov and Sporns, NeuroImage, 52(3):1059–1069, 2010. **[3]** Hagmann et al., PLoS ONE, 2(7):e597, 2007. **[4]** Vaessen et al., NeuroImage, 51(3):1106-1116, 2010. **[5]** Desikan et al., NeuroImage, 31(3):968–980, 2006. **[6]** Fischl et al., Neuron, 33(3):341–355, 2002. **[7]** Parker et al., JMRI, 18(2):242–254, 2003.